Characterization of borides in Co-Re-Cr-based high-temperature alloys

M. Paulisch[1], N. Wanderka[1], G. Miehe[3], D. Mukherji[2], J. Rösler[2] J. Banhart[1]

[1]Helmholtz Zentrum Berlin für Materialien und Energie, Hahn-Meitner-Platz 1, 14109 Berlin, Germany

[2]Technische Universität Braunschweig, Institut für Werkstoffe, 38106 Braunschweig, Germany

[3]Technische Universität Darmstadt, Fachbereich Material- und Geowissenschaften, Petersenstr. 23, 64287 Darmstadt, Germany

*Corresponding author: _wanderka@helmholtz-berlin.de_; Tel.: +49 30 8062 42079; Fax: +49 30 8062 43059

Abstract

Co-Re-Cr- based alloys with additions of 200 ppm or 1000 ppm boron were investigated by high-resolution methods such as scanning electron microscopy, transmission electron microscopy and three-dimensional atom probe. The chemical composition of borides with a lamellar structure resembling a eutectic as determined by three-dimensional atom probe is $Cr_{0.68}Re_{0.46}Co_{0.24}B$, the composition of isolated boride particles at the grain boundaries is $Cr_{0.76}Re_{0.40}Co_{0.35}B$. A systematic study was carried out to determine the crystal structure of the various types of borides. Despite their varying chemical composition, the borides in the two alloys, even when appearing in different morphologies, exhibit the same orthorhombic C-centred unit cell with lattice parameters a = 0.436 nm, b = 0.755 nm and c = 1.498 nm.

1. Introduction

The efficiency of a gas turbine directly depends on the gas entry temperature. The key to higher temperatures and hence better performance is the material of the first stage blades that are subjected to the most stringent conditions of both temperature and loading. In modern gas turbines Ni-based superalloys dominate in the hot sections. However, they already operate close to their temperature limit there. The exploration of new metallic systems for very high temperature applications is therefore an urgent challenge in materials science today. One approach is the examination of a new class of alloys based on the solid solution of cobalt and rhenium [1].

The refractory metal Re has the 3rd highest melting point (3186°C) of all elements, which is an important prerequisite for a potential high-temperature material. The melting point and the degree of solid solution strengthening can be easily tuned by adjusting the Re content. Further alloying additions such as Cr, Si, Ta, Ni or C impart strength and oxidation resistance to Co-Re-based alloys [2, 3]. The ternary alloy Co-17Re-23Cr (composition in at.%) is an experimental reference alloy of the Co-Re system where Cr is added to improve the oxidation behavior of the alloy by promoting the formation of protective Cr_2O_3 oxide layers. However, addition of Cr to Co-Re alloys can also stabilize the Cr-Re-rich (Cr_2Re_3 type) σ phase in the alloy [4], but the σ phase does not make the alloy inherently brittle. Moreover, in the polycrystalline state the alloy is brittle due to grain boundary failure [5]. A similar problem is known in polycrystalline and directionally solidified (DS) Ni alloys, but this has been fixed by adding small amounts of boron 0.5 to 1.0 (at.%) that significantly toughen the material, the reason of which is not yet fully understood [6].

Recently the effect of boron was investigated in Co-17Re-23Cr-based alloys containing between 50 to 1000 ppm B (by mass) [7]. Boron was detected in small (250 nm to 1000 nm) inter-granular particles by electron energy loss spectroscopy (EELS) in the transmission electron microscopy (TEM) and identified by selected area electron diffraction (SAED) as $(Cr,Re)_2B$ phase containing traces of Co [8]. It was reported that the amount of Cr_2B-type particles increases with the boron concentration in the alloy [5, 8].

In the current work, the same Co-17Re-23Cr alloys containing either 200 or 1000 ppm (wt.%) boron were further characterized in more detail. The chemical compositions of the major elements in the different phases were measured by energy dispersive X-ray (EDX) spectroscopy in the TEM and by three-dimensional atom probe (3D-AP). The structure of the boron-rich precipitates was determined using SAED. We discuss these results and compare them with the earlier findings.

2. Experimental

Two Co-17Re-23Cr-based alloys with different boron levels, namely 200 and 1000 ppm (wt.%) were manufactured at the Institut für Werkstoffe, Technische Universität

Braunschweig. The alloys were melted in a vacuum arc furnace and cast into solid copper molds. Solution heat treatment was carried out in a vacuum furnace at 1350°C for 7.5h and at 1400°C for 7.5h, followed by fast cooling with argon gas.

For scanning electron microscopy, small slices of $15 \times 3 \times 0.3$ mm^3 were cut from the cast and heat treated bars and ground to a thickness of 120 µm. In order to visualize the different phases in SEM, selective etching was done using an electrolyte containing 95% acetic acid and 5% perchloric acid. Discs of 3 mm diameter were electropolished by a Tenupol twin jet polishing instrument at +20°C and 35 V. SEM was carried out in a Zeiss 1540 EsB CrossBeam® microscope. Thin foils for TEM were prepared by uniformly electropolishing all phases in a solution of 600 ml methanol, 440 ml butoxyethanol, 60 ml perchloric acid and 7 g carbamide at –28°C and 21 V. A Philips CM30 TEM operating at 300 kV was used for microstructure imaging and for structure analysis using SAED. For this purpose, the specimens were tilted to several zone axes, after which the corresponding SAED patterns from the diffracting Cr boride particles were uniquely indexed by noting the tilting direction (positive or negative) in the microscope. The EDX detector of the TEM was used for chemical composition analysis of the different phases.

Light elements such as boron cannot be quantified by EDX, which is why they were analyzed by means of 3D-AP. Samples for 3D-AP measurements were first polished mechanically. The polished surface was examined by SEM in order to locate B-rich precipitates to which the FIB-based *in-situ liftout* technique could be applied [9-11]. A lamella with the size of about $1.5 \times 10 \times 6$ µm^3 was lifted out and positioned at the end of a Mo tip which had been electrolytically processed to a diameter of 1.5 µm before. In order to prepare thin needles suitable for 3D-AP analysis with a radius below 50 nm from the actual sample containing the selected B-rich precipitates at the apex, specimen sharpening was performed using annular-pattern milling in the Zeiss 1540EsB CrossBeam® workstation. Final milling was done using a beam current of 20 pA down to 10 pA in order to minimize Ga implantation. The 3D-AP analyses were performed at 10^{-8} Pa pressure and a temperature of 70 K with a 20 % pulse fraction and a pulse repetition rate of 1 kHz. A tomographic atom probe from CAMECA was used in the present 3D-AP investigations [12].

3. Results and Discussion

3.1 Microstructure

3.1.1 Co-17Re-23Cr+200B alloy

The microstructure of the Co-17Re-23Cr+200B alloy as imaged by SEM is shown in Fig. 1. Several globular σ phase particles (~10 µm) in size embedded in the matrix of the Co-solid solution grains are seen in Fig. 1a. The grain boundaries and some of the particles are decorated by borides. Due to preferential etching of the matrix it is possible to visualize the borides covering the σ phase particles very clearly, see Fig. 1b. The borides are Cr-rich with lamellar structure resembling a eutectic morphology (Fig. 1b).

More details of these phases are revealed by TEM. σ phase particles of different sizes as well as some small boride particles at the σ interfaces appear in Fig. 2 and confirm the observation by SEM that the σ phase and the borides are associated with each other. This association, however, is observed only for the large σ phase particles shown in Fig. 2a but not for the smaller ones in Fig. 2b. Small σ particles are more polygonal, whereas the larger σ particles are more globular in shape. The chemical compositions (with the exception of B) of the matrix, the σ phase and the boride phase as measured by EDX in the TEM are listed in Table 1. The chemical compositions of the borides located at the grain boundaries or at the σ interfaces are nearly the same and listed in Table 1.

3.1.2 Co-17Re-23Cr+1000B alloy

A higher amount of B (1000 ppm) significantly changes the microstructure of the alloy (Fig. 3a). No σ phase is present any more and a larger amount of borides compared to the alloy with 200 ppm B is observed. Borides are mainly located at the grain boundaries but some also in the grain interior. Most of the grain boundaries are now decorated with isolated boride particles but also accumulations of borides are found within the grains. The lamellar structure of the borides is well resolved even in the low-magnification SEM image (Fig. 3b) owing to strong contrast between matrix and the precipitates caused by the edge effect of the protruding boride precipitates in the etched alloy. SEM images show that the borides have a morphology similar to a eutectic in regions where they cluster, with inter-lamellar distances of below 2 μm (Fig. 3b). A TEM image of the borides (marked by arrows) with said lamellar structure near the grain boundaries is shown in Fig. 3c. The composition of the matrix and of two types of borides (isolated and lamellar) as measured by TEM-EDX is displayed in Table 1.

The compositions of several isolated as well as lamellar borides in alloy Co-17Re-23Cr+1000B were also analyzed by 3D-AP. The compositions along with that of the matrix are listed in Table 1. Figure 4a shows the three-dimensional reconstruction of B, Re and Cr atom positions in a small analyzed volume at the interface between boride and the matrix. The positions of Co atoms are omitted for clarity. The corresponding depth profiles of all alloying elements along a cylinder with a radius of 1 nm located in the center of investigated volume are shown in Fig. 4b. This figure reveals significant enrichment of B at the interface. The microstructures of both boron-containing alloys obtained in the present work are consistent with those reported by Bölitz et al. [8].

The chemical composition of the matrix in both alloys is the same considering the experimental error, whereas those of the borides with various morphologies differ (see Table 1). Due to the absence of the σ phase in the alloy containing 1000 ppm B a redistribution of alloying elements between the different phases must have taken a place.

According to the chemical composition the σ phase contains only half the Cr that is present in the Cr borides. Since the Cr content in the matrix of both B-containing alloys is the same

within the experimental error, it is near at hand that the entire Cr in the alloy with 1000 ppm B which would otherwise be in the σ phase (as in the alloy with 200 ppm B) actually partitions to the boride phase. This result is not unusual, since it has been reported that B has a strong affinity for Cr and Re [13]. Even a 50 ppm B addition to Co-Re alloys results in the precipitation of Cr boride. Furthermore, in some Co-Re alloys containing Cr carbides the B also interacts with these carbides. Similar observations have been reported in some Cr-rich stainless steels. Thus, the addition of B to Co-Re alloys apparently influences the partitioning of Cr and Re in this alloy system and thereby can influence phase formation and stability.

The Re content of the matrix in the alloy with 1000 ppm B is a little higher than in the alloy with 200 ppm B, see Table 1. Hence, most of the Re which was in the σ phase is used for boride formation in the high-boron alloy and it does not partition to the matrix. Comparing the boride precipitates with different morphologies in the high-B alloy, it is seen that the Re content in the isolated borides at the grain boundaries is lower than in the lamellar borides. Moreover, the Co content in the matrix at the grain boundaries as well in the isolated borides is higher than in the matrix region far away from the grain boundaries. One explanation could be that Co substitutes Re in these areas at the grain boundary.

The chemical compositions of different phases in Co-17Re-23Cr+1000B and in particular of the borides were measured by 3D-AP for the first time. These compositions along with that of the matrix are listed in Table 1. As an example of 3D-AP measurements, the reconstruction of B, Re and Cr atom positions at the interface between an isolated boride and the matrix in a small volume is given in Fig. 4a. The positions of Co atoms are omitted for the sake of clarity. The corresponding depth profiles of all alloying elements along a cylinder with a radius of 1 nm located in the center of investigated volume are shown in Fig. 4b. This figure reveals significant enrichment of B at the interface. On the matrix side near the interface the concentration of Co is lower than in the matrix (see Table 1) whereas the amount of Cr remains constant. No B could be detected in the matrix by 3D-AP. This agrees with the observations by Bölitz et al. who however, presented a boride phase composition of $CrRe_{0.7}Co_{0.3}B$, which represents a stoichiometric Cr_2B-type boride [8]. We determine the compositions of the lamellar and isolated borides as $Cr_{0.68}Re_{0.46}Co_{0.24}B$ and $Cr_{0.76}Re_{0.40}Co_{0.35}B$, respectively. Compositions of the borides found in the present study are off-stoichiometric and contain less metal than the M_2B phase.

3.2 Structure Analysis of the Boride Phase

The crystal structures of the isolated as well as of the lamellar Cr-borides were determined by SAED. Both types have the same crystal structure [14]. The boride particle chosen for SAED analyses was located at a grain boundary. Exemplary SAED patterns of the boride phase in the Co-17Re-23Cr+1000B alloy obtained in three different zone axes are shown in Fig. 5.

The diffraction pattern shown in Fig. 5a suggests hexagonal symmetry. The volume of the supposed hexagonal cell can be estimated from the diameter of the 1st order Laue zone in

Fig. 5a (outside the depicted area), which gives a preliminary value for the volume of the reduced cell and indicates that the cell is primitive. The zones shown in Fig. 5b and 5c were used for the accurate determination of the lattice parameters. Within the experimental accuracy, the metric of the basic parallelogram in Fig. 5b is the same as that in Fig. 5c, but the intensities are different. The d-values obtained from these patterns were included in a refinement process. The lattice parameters of a hexagonal primitive cell were found to be $a_h = 0.436(4)$ nm and $c_h = 1.498(15)$ nm. Applying these parameters, Figs. 5b and 5c represent zones [-111] and [121], respectively. The arrangement of the weak diffraction spots in Fig. 5b, however, contradicts hexagonal or trigonal symmetry but is compatible with an orthorhombic C-centred cell with the lattice parameters $a = a_h = 0.436(4)$ nm, $b \approx a_h \sqrt{3} = 0.755(6)$ nm and $c = c_h = 1.498(15)$ nm. In term of this cell the three zones in Fig. 5 are [001], [-312], and [011], respectively. The cell parameters were confirmed by comparing observed and calculated angles between the three zone axes.

With respect to the intensity of the diffraction spots two parity groups can be clearly distinguished in Fig's. 5a and 5b: on the one hand, strong reflections with h,k,l all odd or all even and, on the other hand, weak ones with odd and even indices mixed. The strong reflections indicate an F-centred subcell. In zone [001] (Fig. 5a) the strong reflections $hk0$ fulfil the extra condition $h+k=4n$. This suggests that the space group of the subcell has to be either $F2dd$ or $Fd2d$ (both no. 43) or $Fddd$ (no. 70). $Fddd$ is the space group of Cr_2B (CuMg$_2$-type). The lattice parameters of Cr_2B are $a = 0.4275$ nm, $b = 0.7452$ nm, $c = 1.4795$ nm, $Z = 16$ [15], which is very close to those of the orthorhombic C-centred cell. This suggests that the structures are closely related.

The chemical composition of the Cr-boride phase as measured by 3D-AP and listed in Table 1 shows that the amount of boron exceeds that of the stoichiometric Cr_2B phase. It is found close to $(Cr,Re,Co)_3B_2$. Cr, Re, Co and B relate approximately as 6:3:3:8. The CuMg$_2$ structure type applies to the boride phase. This means that Co, Re or Cr atoms are partially substituted by B atoms. Based on the composition given in Table 1 the phase can be expressed as $(Cr_{0.91}Re_{0.48}Cr_{0.42}B_{0.19})B$.

The violation of F-centring is due to an – at least partial – ordering of the species Co, Re, Cr and B. The amount and quality of data obtained experimentally (Fig. 5) is not sufficient to derive details of occupancy or even of the associated shifts of the positional parameters.

Any proposal for a potentially correct structure has to satisfy two conditions. First, the pseudo-hexagonal symmetry of zone [001] has to be preserved, at least for the strong reflections. Second, simulations have to reproduce the classification of strong and weak reflections.

C-centred *klassengleiche* subgroups of $Fddd$ are the non-centrosymmetric space groups $C222$ (No.21) and $C222_1$ (No.20). With space group $C222_1$ it is impossible to meet both conditions simultaneously. There are, however, possibilities within space group $C222$. Table 2a gives the parameters for the $Fddd$ structure of Cr_2B and Table 2b the parameters of the same structure expressed in terms of space group $C222$. From now on, (Co,Re,Cr,B) is named "M"

followed by two indices. The first index (1 or 2) refers to the number of the Cr atom in Cr_2B (Table 2a) from which M has emerged, the second one is a consecutive number.

While 3 free positional parameters are sufficient to describe the structure of Cr_2B in space group *Fddd* (two Cr sites, one B site), 13 parameters are available in space group *C*222 (seven M sites and four B sites). The most important free parameters are the relative scattering powers of the M sites, named "F(M)" in the following. If F takes the same value for all M sites this makes the structure of Cr_2B the reduced cell of which is outlined in Fig. 6 by dashed lines. If F(M11) = F(M12) = F(M13) and F(M21) = F(M22) = F(M23) = F(M24), the symmetry is still *Fddd*, i.e. weak reflections are absent. Introducing the auxiliary conditions F(M12) = F(M13) and F(M22)+F(M24) = 2·F(M23) and leaving F(M11) and F(M21) unconstrained preserves the hexagonal symmetry of zone [001]. The "weak" reflections occur as soon as F(M11) differs from F(M12) or F(M21) differs from F(M22). A second model which is generated if, in the above conditions, M12 is replaced by M11 and M23 by M21, is not identical but equivalent.

There is no completely ordered distribution of the four species Cr, Co, Re and B on the seven M sites (one site – one element) which would meet the measured composition 6:3:3:8 and fulfil the auxiliary conditions. Therefore, mixed occupancies have to be assumed. The results of model calculations are ambiguous. It is not even possible to decide whether, e.g., F(M21):F(M23) is < 1 or >1.

The findings from the above considerations are:

(i) A set of start parameters (Table 2b) for future refinements of the structure based on more and better data,

(ii) The evidence of mixed site occupancies and,

(iii) Some relationships between mixed site occupancies expressed by the auxiliary conditions.

The fact that the structure is non-centrosymmetric might also be of interest.

Despite the differences in composition both types of borides studied in the alloys with 200 and 1000 ppm B have the same crystal structures. This implies that this phase has a large range of existence in the phase diagram.

Bölitz et al. postulated Cr_2B as the composition of the borides and derived an orthorhombic structure with space group *Fddd* [8] in analogy to the structure and space group of the pure Cr_2B phase [15]. In our more detailed investigation we find that the boride phase also include Re atoms in addition to Cr and B. La Placa et al. [16] found by XRD that Re_2B has a centrosymmetric *P*6/*mmc* structure. Therefore, Cr_2B and Re_2B have different symmetries. Our more detailed investigations reveal that the structure of the Cr-Re-borides exhibits a *C*-centred orthorhombic unit cell which belongs to space group *C*222 (no. 21). As described above, the *C*-centred structure of the borides fulfils the conditions of occurrence of all diffraction patterns with strong and weak reflections obtained in SAED images.

Re_2B has an orthorhombic crystal structure with space group *Cmcm* (no. 63) [17, 18]. In the Co-17Re-23Cr+B alloys investigated in this study, the boride phase is rich in Cr and Re with some Co. Due to the high rhenium content in the Cr borides it is likely that rhenium influences structure formation. Partial ordering of the Re atoms changes the symmetry from *F*-centred in Cr_2B to *C*-centred in $Cr_{0.68}Re_{0.46}Co_{0.24}B$ and $Cr_{0.76}Re_{0.40}Co_{0.35}B$ phases.

4. Conclusions

Boron additions of 200 or 1000 ppm to the alloy Co-17Re-23Cr have a pronounced influence on its microstructure. The alloy with the lower B amount contains stable σ phase precipitates as it is the case without B addition. Borides at the grain boundaries are formed. For higher B content, the σ phase is no more stable and the Cr-Re-rich borides have a different morphology compared to the alloy containing only 200 ppm boron. As the σ phase and the borides are both rich in Cr and Re, the stability of the different phases in alloys with different boron contents can be attributed to the higher affinity of Cr to B.

3D-AP was used to measure the chemical compositions of borides in Co-Re alloys. The compositions of the two boride morphologies, namely lamellar (eutectic-like) borides and isolated boride particles were slightly different, but their crystal structure was the same.

The Cr-Re-borides in both these morphologies contain less metal than stoichiometric M_2B which contradicts an earlier report in the literature, where Cr-Re-boride in Co-17Re-23Cr+B alloys was reported to be stoichiometric Cr_2B type. The present study finds that both Cr and Re are present in the boride phase. It is known that Cr_2B and Re_2B have different structures. The orthorhombic *C*-centred structure with lattice parameters a = 0.436 nm, b = 0.755 nm and c = 1.498 nm describes best the Cr-Re-rich boride found in the present study. It is a superstructure of the *F*-centred binary Cr_2B structure.

Acknowledgments

References

[1]   J. Rösler, D. Mukherji, T. Baranski, Adv. Eng. Mater. 9 (2007) 876-881

[2]   M. Klauke, D. Mukherji, B. Gorr, H.–J Christ, J. Rösler, Int. J. Mat. Res., 100 (2009) 104-111

[3]   B. Gorr, V. Trindade, S. Burk, H.-J. Christ, M. Klauke, D. Mukherji, J. Rösler, Oxid. Metal, 71 (2009) 157-172

[4]   D. Mukherji, P. Strunz, R. Gilles, M. Hofmann, F. Schmitz, J. Rösler, Mater. Lett. 64 (2010) 2608-2611

[5]   D. Mukherji, J. Rösler, M. Krüger, M. Heilmaier, M.-C. Bölitz, R. Völkl, U. Glatzel, L. Szentmiklósi, Scripta Mater. 66 (2012) 60-63

[6]   B.C. Yan, J. Zhang, L.H. Lou, Mat. Sci. Eng. A 474 (2008) 39-47

[7]   D. Mukherji, J. Rösler, J. Wehrs, P. Strunz, B. Přemysl, R. Gilles, M. Hofmann, M. Hoelzel, H. Eckerlebe, L. Szentmiklósi, Z. Mácsik, Metall. Mater. Trans. 43A (2012), in print: DOI: 10.1007/s11661-012-1363-6

[8]   M-C. Bölitz, M. Brunner, R.Völkl, D. Mukherji, J. Roesler, U. Glatzel, Int. J. Mater. Res. 103 (2012) 554-558

[9]   K. Thompson, D. Lawrence, D.J. Larson, J.D. Olson, T.F. Kelly, B. Gorman, Ultramicroscopy 107 (2007) 131-139

[10]   M.K. Miller, K.F. Russel, G.B. Thompson, Ultramicroscopy 102 (2005) 287-298

[11]   D.W. Saxey, J.M. Cairney, D. McGrouther, T. Honma, S.P. Ringer, Ultramicroscopy 107 (2007) 756-760

[12]   D. Blavette, B. Deconihout, A. Bostel, J.M. Sarrau, M. Bouet, A. Menand, Rev. Sci. Instrum. 64 (1993) 2911-2919

[13]   M. Hoyer, Dissertation, Technische Universität Chemnitz (2005)

[14]   M. Paulisch, Diploma Thesis, Technische Universität Berlin (2011)

[15]   D. Kotzott, M. Ade, H.Hillebrecht, Solid State Science, 10 (2008) 291-302

[16]   S. La Placa, B. Post, Acta Cryst. 15 (1962) 97-99

[17]   K.I. Portnoi, V.M. Romashov, Translated from Poroshkovaya Metallurgiya 2 (1968) 41-44, Original article submitted September 8 (1966)

[18]   V.S. Telegus, Yu.B. Kuz'ma and Ts. K. Stefanishina, Powder metal. Met. C 8 (1969) 133-136
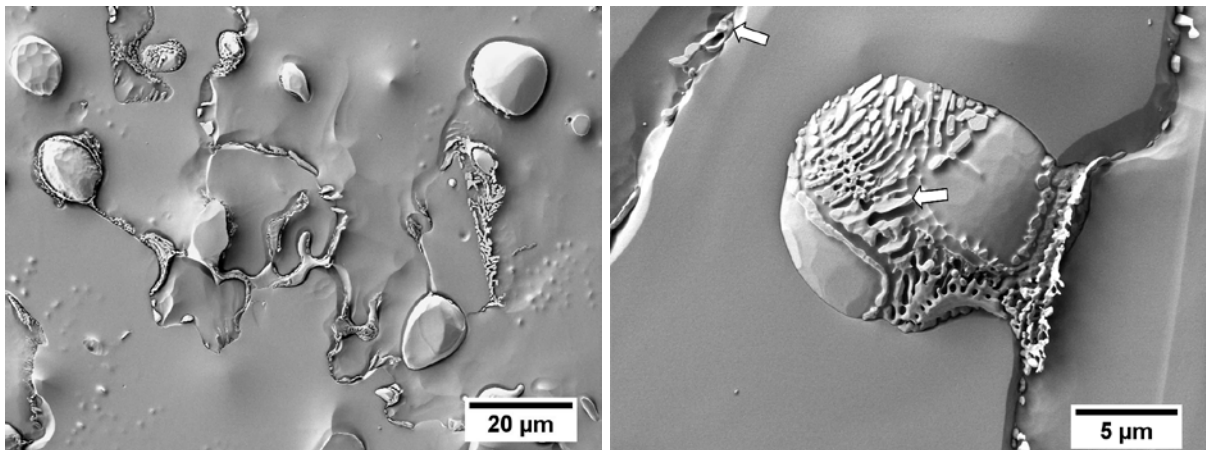
Figures

Fig. 1: Secondary electron SEM images of the Co-17Re-23Cr alloy containing 200 ppm B: (a) globular σ precipitates embedded in the matrix. Borides with lamellar morphology resembling a eutectic decorate grain boundaries and σ phases. (b) close-up of such borides at a grain boundary and a σ precipitate, both marked by an arrow.
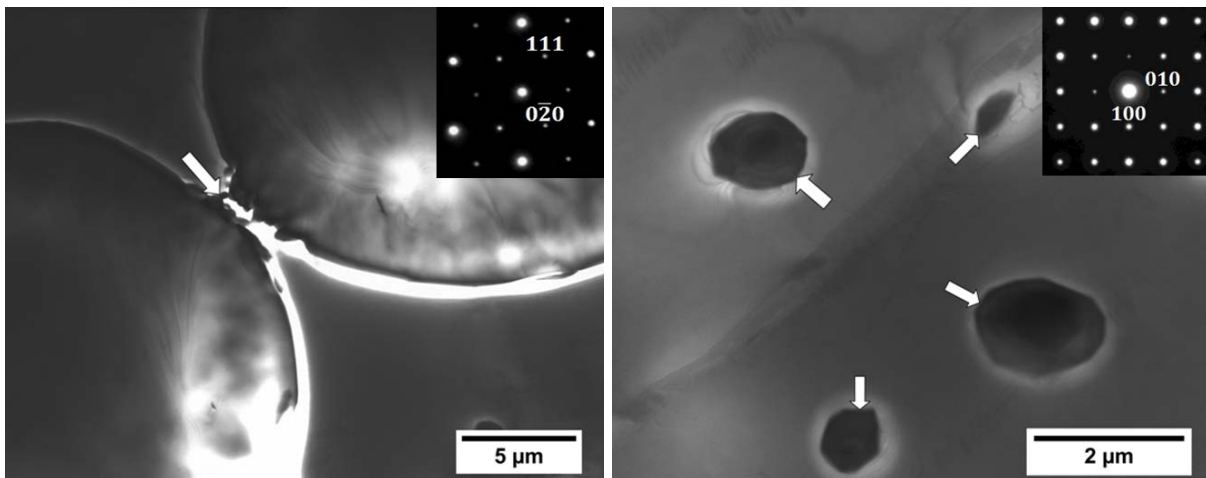

Fig. 2: BF TEM images of Co-17Re-23Cr + 200 ppm B: (a) large σ precipitates surrounded by borides (marked by an arrow); SAED pattern of σ precipitate along the [001] zone axis is shown in the inset. (b) four small σ precipitates (dark, marked by arrows) without boride decoration; SAED pattern of boride along the [-101] zone axis is shown in the inset.
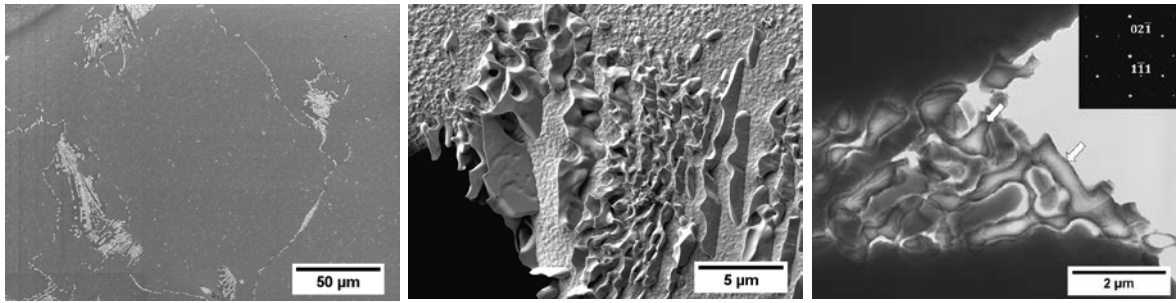
Fig. 3: (a, b) Secondary electron SEM images of Co-17Re-23Cr alloy containing 1000 ppm B. (b) plate-like borides embedded in the matrix. (c) BF TEM image of lamellar structure of boride phases (marked by arrows) within the grain boundary. SAED pattern of boride phase along the [-112] zone axis is shown in the inset.
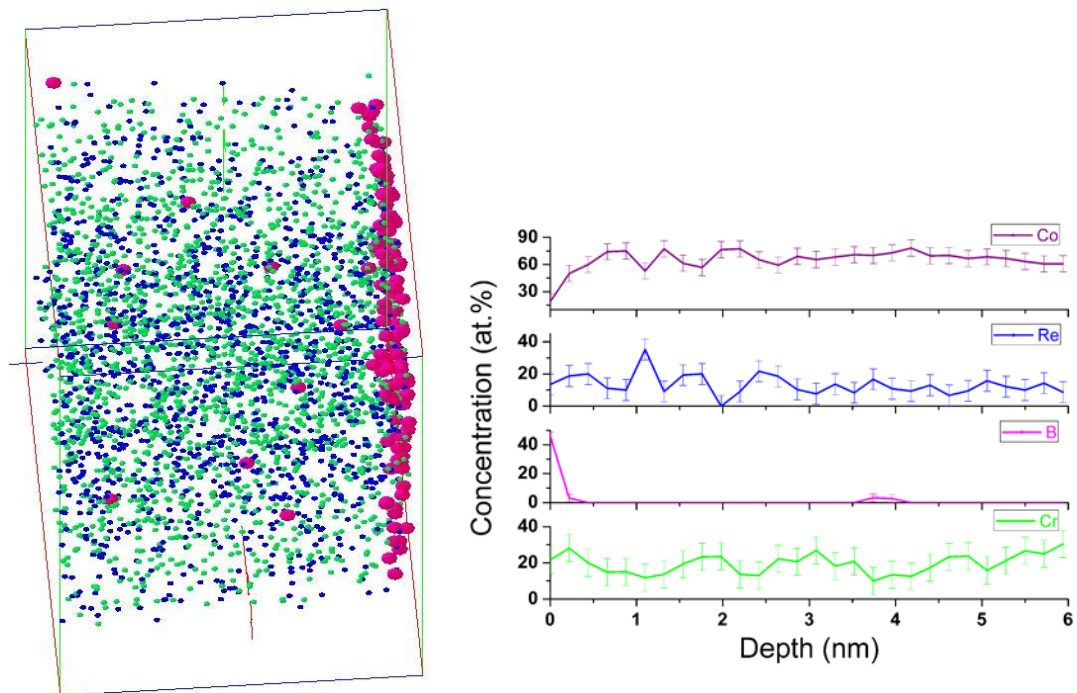

Fig. 4: (a) Three-dimensional reconstruction of atom positions: boron (pink), rhenium (blue) and chromium (green). The analyzed volume in the Co-17Re-23Cr alloy with 1000 ppm B is 8.4 x 8.4 x 6.4 nm^3. (b) Corresponding depth profiles of all alloying elements along a cylinder with radius of 1 nm located at the centre of the volume shown in (a).
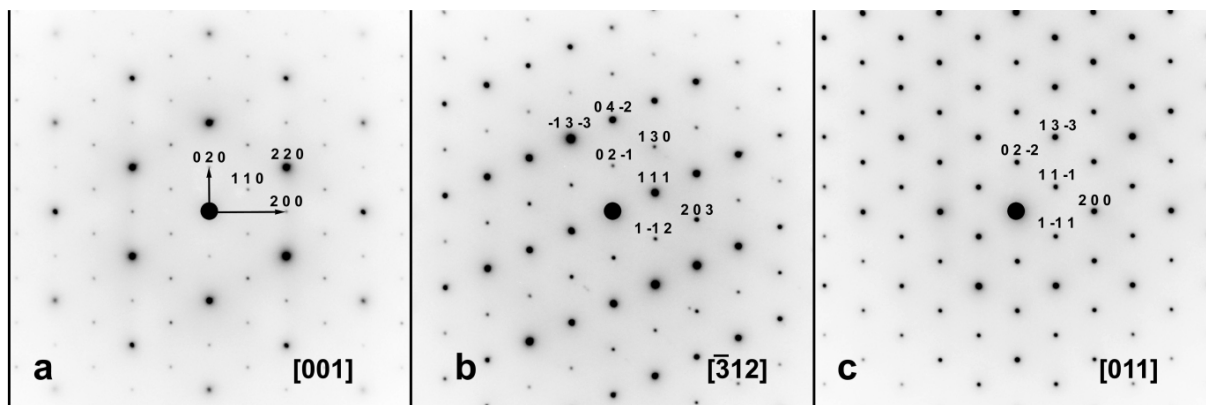
Fig. 5: Selected area electron diffraction patterns of the boride phase ($Cr_{0.91}Re_{0.48}Cr_{0.42}B_{0.19}$)B at the grain boundary of Co-17Re-23Cr+1000B, indexed in terms of the orthorhombic cell with space group $C222$: (a) zone [001], (b) zone [-312] and (c) zone [011].
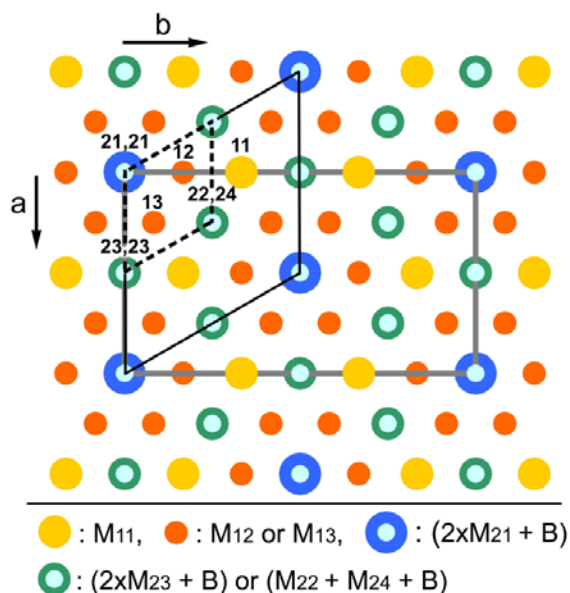

: M_{11}, : M_{12} or M_{13}, : ($2 \times M_{21}$ + B)
: ($2 \times M_{23}$ + B) or (M_{22} + M_{24} + B)

Fig. 6: Crystal structure of ($Cr_{0.91}Re_{0.48}Cr_{0.42}B_{0.19}$)B phase projected along c: the small "hexagonal" cell marked by dashed lines represents the primitive setting of the *Fddd* structure. The big "hexagonal" cell is the primitive setting of the *C*222 cell. The rectangular cell represents the *C*-centred setting. The true symmetry of this projection is *cmm*. The indices of the M sites refer to Table 2b. Sites labelled by two names (e.g. "21,21") represent two overlapping atoms. Bright cores of these sites represent B atoms.

Tables

Table 1: Nominal compositions of the Co-17Re-23C+200B and Co-17Re-23Cr+1000B alloys together with the chemical composition of the phases as measured by TEM-EDX and 3D-AP. All values are given in at.%. The given errors refer to one standard deviation. TEM-EDX does not yield reliable data for B concentration.

Method	Alloy	Phase	Co	Re	Cr	B
	Co-17Re-23Cr + 200 ppm B	nominal composition	59.85	17.0	23.0	0.15
	Co-17Re-23Cr + 1000 ppm B	nominal composition	59.27	17.0	23.0	0.73
TEM	Co-17Re-23Cr + 200 ppm B	matrix	63.2 ± 0.7	14.6 ± 0.5	22.2 ± 0.4	
		σ phase	39.2 ± 1.0	27.5 ± 0.7	33.4 ± 1.3	
		borides at grain boundaries	11.8 ± 1.5	34.4 ± 1.9	53.9 ± 0.9	
		borides near σ interface	10.6 ± 0.3	34.2 ±0.9	55.3 ± 1.0	
	Co-17Re-23Cr + 1000 ppm B	matrix	62.8 ± 2.3	16.6 ± 1.3	20.6 ± 1.3	
		matrix between boride lamellas	69.4 ± 1.0	11.5 ± 1.2	19.2 ± 0.6	
		boride, isolated	25.3 ± 1.5	25.4 ±1.0	49.3 ± 0.6	
		boride, lamellar structure	18.4 ± 2.1	34.2 ± 1.6	47.5 ± 1.1	
3D-AP	Co-17Re-23Cr + 1000 ppm B	matrix between boride lamellas	68.7 ± 0.5	13.7 ± 0.3	17.6 ± 0.4	-
		boride, isolated	14.0 ± 0.2	16.1 ± 0.2	30.2 ± 0.3	39.8 ± 0.3
		boride, lamellar structure	9.9 ± 0.2	19.5 ± 0.3	28.7 ± 0.3	41.9 ± 0.4
		boride interface, isolated	10.4 ± 2.5	14.6 ± 2.9	32.6 ± 3.9	42.4 ± 3.9

Table 2: The structure of the phase Cr_2B: Positional parameters of representations (a) in space group *Fddd* (data from [15]) and (b) in space group *C*222. For the meaning of the atom species "Mi_1i_2" see text.

space group C 2 2 2 (#21)

Cr_2B, $a = 0.4275$ nm, $b = 0.7452$ nm, $c = 1.4795$ nm

space group *F d d d* (#70)

atom	x	y	z	Wyck	free
Cr(1)	0	0.333	0	16 f	y
Cr(2)	0	0	0.083	16 g	z
B	0	0	0.375	16 g	z

sites: 3, free positional parameters: 3

atom	x	y	z	Wyck	free
M11	0	0.333	0	4 g	y
M12	0	0.833	1/2	4 h	y
M13	0.250	0.583	0.250	8 l	x y z
M21	0	0	0.083	4 i	z
M22	1/4	1/4	0.167	4 k	z
M23	0	1/2	0.583	4 j	z
M24	1/4	1/4	0.333	4 k	z
B1	0	0	0.375	4 i	z
B2	1/4	1/4	0.875	4 k	z
B3	0	1/2	0.875	4 j	z
B4	1/4	1/4	0.625	4 k	z

sites: 11, free positional parameters: 13

(a)   (b)